On shapes and forms: Population balance dynamics of corrugated stirred fronts

Des formes et des contours : une dynamique de population pour les fronts agités

Emmanuel Villermaux [a,b,c,*]

[a] *Aix Marseille Université, CNRS, Centrale Marseille, IRPHE UMR 7342, Marseille, France*
[b] *Institut universitaire de France, Paris, France*
[c] *CNRS/MIT/AMU Joint Laboratory "MultiScale Materials Science for Energy and Environment", MIT Energy Initiative, Massachusetts Institute of Technology, Cambridge, MA 02139, USA*

ARTICLE INFO

ABSTRACT

We introduce a unified framework to discuss the emergence of corrugations on material interfaces transported by random media. Relating the shape of these interfaces to the stirring field giving birth to it, we formalize a population balance dynamics for the r-elements (segments of length r) needed to cover the interface contour in the course of its deformation. As long as corrugations grow kinematically, shapes change continuously, their fractal dimension $d_f(r,t)$ is a non-monotonous function of the scale r, and increases in time t with no bounds. Interface creation and destruction balance, however, in self-propagating fronts like flames, and in fronts smearing by molecular diffusion, through a mixing induced overlap mechanism, leading to a stationary shape. These findings, which help reexamining old observations in a new perspective, also reconcile kinetics with geometry.

RÉSUMÉ

Nous introduisons un cadre unifié pour discuter l'émergence de corrugations sur les interfaces matérielles transportées dans des milieux agités aléatoirement. En reliant la forme de ces interfaces au champ d'agitation qui la crée, nous formalisons une dynamique de bilan de population pour les r-éléments (segments de longueur r) nécessaires pour couvrir le contour de l'interface au cours de sa déformation. Tant que les corrugations croissent cinématiquement, les formes changent continuellement, leur dimension fractale $d_f(r,t)$ est une fonction non monotone de l'échelle r et augmente dans le temps t sans limite. La création et la destruction d'interfaces s'équilibrent toutefois pour les fronts auto-propagés tels que les flammes, et pour les fronts qui s'étalent par diffusion moléculaire, par un mécanisme de chevauchement induit par le mélange, conduisant à une forme

---

* Correspondence to: Aix Marseille Université, CNRS, Centrale Marseille, IRPHE UMR 7342, Marseille, France.
E-mail address: emmanuel.villermaux@univ-amu.fr.

stationnaire. Ces résultats, qui permettent de réexaminer d'anciennes observations dans une nouvelle perspective, réconcilient également la cinétique avec la géométrie.

1. Introduction

> Ce qui est réel, c'est le changement continuel de forme :
> la forme n'est qu'un instantané pris sur une transition.
> Henri Bergson (1907), *L'évolution créatrice*

Our aim is to describe the shape of interfaces, contours, lines, and surfaces transported by moving continuous media, and to relate this shape to the process giving birth to it, namely to a feature of the motion itself. Our examples are mostly in fluids, although the discussion is not restricted to any kind of medium in particular. We will only need the motions to have a velocity field such that its velocity increments $v(r)$, that is, the mean separation velocity of two points in the medium distant by r is known, and is statistically steady in time (i.e. depends on r only). We call it the stirring field.

Our definition of the 'shape' is such that it should be related to the stirring field. Since the latter is r-dependent, we will call the shape of the interface the relationship existing between the number $N(r,t)$ of segments of length r needed to cover it versus r at a given time t as (Fig. 1a),

$$N(r,t) \sim \left(\frac{R}{r} \right)^{d_{\mathrm{f}}} \tag{1}$$

where R is an outer scale defining the total extend of interface, and d_{f} is a fractal dimension [1]. Accordingly, the net length of the interface measured at scale r is

$$L(r,t) \sim r N(r,t) \tag{2}$$

while a surface embedded in the three-dimensional space has an area $r^2 N(r,t) \sim r^{2-d_{\mathrm{f}}}$.

Enforcing a strict power-law dependence on r in (1) does not imply that d_{f} will, in general, be a constant number. In fact, depending on the precise form of $v(r)$, and depending if the interface has reached a steady state, or if it is developing in time t, the dimension $d_{\mathrm{f}}(r,t)$ will be shown to be generically dependent on both r and t.

The question envisaged here is not new. In a celebrated paper, G. I. Taylor [5] established a connection between the velocity fluctuations and the dispersion of a *single* particle in turbulent flows, making this way a remarkable (but unnoticed at that time) parallel with Langevin's method to describe thermally activated diffusion [6]. L. F. Richardson related the structure of the velocity differences $v(r)$ to the scale-dependent dispersion coefficient of *pairs* of particles in a not less celebrated (and unnoticed at the time, see [7]), contribution [8].

However the status of the shape of material lines and surfaces (and not only the dispersion properties of their constitutive particles) in stirred, random or turbulent media was only considered much later (see, e.g., [2,9]), and notably by the time the concept of *fractals* became popular (see [10] for a review). For instance, it was argued that the shape of the stationary surface separating a turbulent from a non-turbulent medium has a dimension $d_{\mathrm{f}} = 7/3$ (or $4/3$ when the surface is intercepted by a plane cut as in Fig. 1c) and that this number could be related to Kolmogorov's scaling for $v(r)$ at high Reynolds number. This statement was soon moderated by more refined measurements showing that while $N(r,t)$ is indeed steeper than for a smooth object, it is however not a strict power law in r [11] and is in addition, for a growing interface as in Fig. 1b, time dependent [3,12,13]. Similar ideas to those used to describe fronts passively advected were applied to self-propagating fronts like flames [14] and were criticized too [15,16], including when the intrinsic destabilization of these fronts cooperates to their corrugation [17].

It is our aim to describe the structure of these interfaces beyond the standard, and not always convincing scaling arguments by articulating a relationship between the geometry of the corrugations, and the dynamics ruling their existence, from their birth, to their possible destruction. The objects we will describe are illustrated in Fig. 1. They consist in both arborescent lines (Fig. 1b) and surfaces (Fig. 1c) of passively transported scalar quantities, as well as stationary chemically reactive fronts in turbulent flows (Fig. 1d). For each of these situations, we will decipher the method of construction of $N(r,t)$ in Eq. (1) by computing the scale-by-scale budget of the r-elements covering the interface (Fig. 1a) in relating it to the structure of the stirring field $v(r)$. In this process, it will be seen that the knowledge of the microscopic principles of scalar mixing are required to describe properly the shape of interfaces that dilute, mix, or react in the field distorting them.
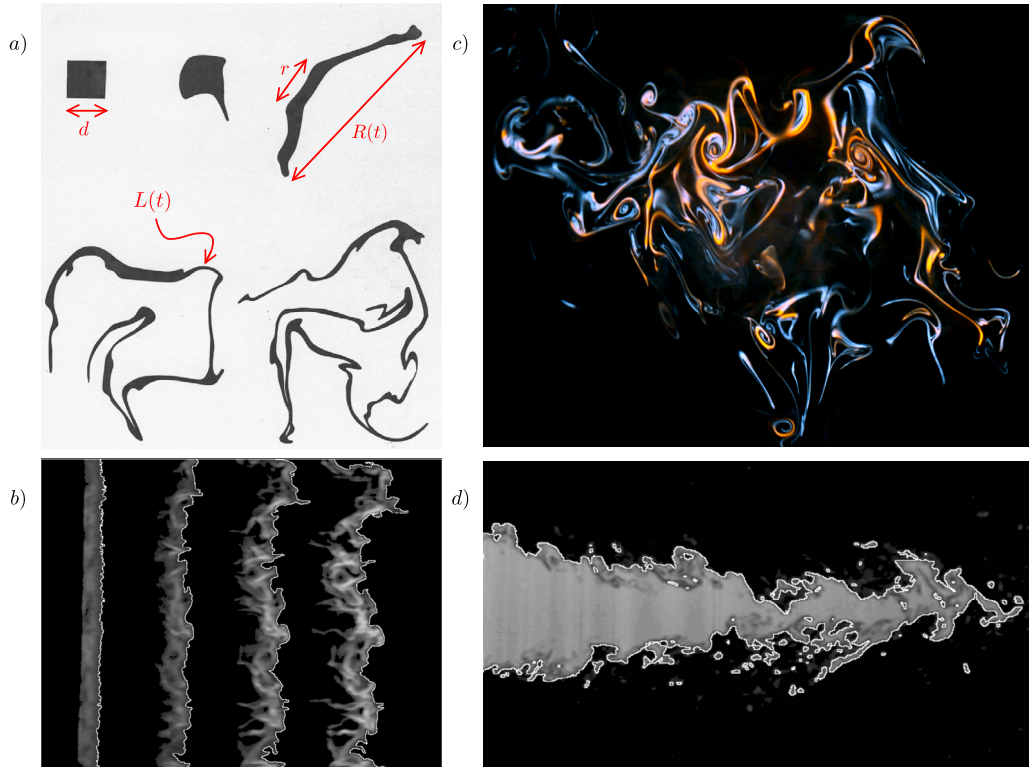
Fig. 1. a) Stirring kinematics of a blob in a flow where the separation velocity $v(r) = \langle \Delta r / \Delta t \rangle$ depends on the separation r itself. The distorted blob net length $L(t)$ is different from the end-to-end dispersion $R(t)$. Adapted from [2]. b) The corrugation of a line transported by a turbulent flow shown at successive instants of time [3]. c) A cut through a compound plume from nearby sources of two different color dyes stirred in a turbulent jet. d) An instantaneous cut on the axis of a neutral (pH = 7) water turbulent jet (4 cm in diameter, the Reynolds number is of order 10^4), seeded with a pH-sensitive fluorescent dye issuing in an acid environment at pH = 2. The fast acid-basic neutralization of the dye occurs on a sharp, corrugated interface [4].

2. Scale-by-scale budget of front corrugations

2.1. Population balance of r-elements

We call $N(r, t)$ the number of segments of length r needed to cover an interface contour at time t (see Fig. 1a). Because the substrate supporting the interface is stirred, and because the segments are delimited by material points carried by the flow, each segment is, in the mean, stretched by the base flow by an amount Δr during the time interval Δt. Conservation of the number of segments that transit under stirring from r to $r + \Delta r$ during Δt writes [3]:

$$N(r + \Delta r, t + \Delta t) = N(r, t) - \dot{N}(r, t)\big|_{\text{loss}} \Delta t \tag{3}$$

giving, on ensemble average,

$$\partial_t N + \left\langle \frac{\Delta r}{\Delta t} \right\rangle \partial_r N = - \dot{N}(r, t)\big|_{\text{loss}} \tag{4}$$

where $\dot{N}(r, t)\big|_{\text{loss}}$ is a possible sink term that represents the rate of destruction of r-elements either by diffusive reconnection between nearby elements, or erasing by front propagation, as we will see.

Central to the population balance dynamics of $N(r, t)$ is thus the r-dependence of the separation (or pair dispersion) velocity $\langle \Delta r / \Delta t \rangle$ between two material points separated by r. This velocity is in practice affected by fluctuations inducing exchanges between neighboring r-classes in the population $N(r, t)$. These are reflected by a non-zero $\langle \Delta^2 r / \Delta t^2 \rangle$ term at the next order in Eq. (4), giving rise to a lognormal distribution of stretching factors in random flows [18,19]. However, the present discussion only requires the knowledge of the r-scaling of $\langle \Delta r / \Delta t \rangle$, irrespective of its fluctuations.

2.2. Stirring law

In nature, the separation velocity $\langle \Delta r / \Delta t \rangle$, may it concern time-dependent flows like in turbulence [3], or stationary flows like in random porous media [20] for instance, always presents a crossover between a simple shear dominated régime,

and a régime with a scaling dependency either enforced by a conservation law, or by a prescribed geometrical disorder. We call d the characteristic crossover lengthscale, which coincides, for instance, with the Taylor scale in turbulent flows (which marks the frontier with the intermediate dissipative range of scales where viscosity progressively regularizes the motion, down to the Kolmogorow scale, where the motion is essentially damped), or with the pore size in a porous medium, and we make distances r dimensionless as

$$r \equiv \frac{r}{d} \tag{5}$$

A generic expression for the separation velocity $\langle \Delta r / \Delta t \rangle$ suitable for the variety of stirring fields alluded to above is

$$\left\langle \frac{\Delta r}{\Delta t} \right\rangle \quad \equiv \quad v(r) \tag{6}$$

$$= \quad u\,r^{1-\xi}\left(1 - e^{-r^{\xi}}\right) \tag{7}$$

$$\xrightarrow[r \ll 1]{} u\,r \tag{8}$$

$$\xrightarrow[r \gg 1]{} u\,r^{1-\xi} \tag{9}$$

interpolating, through a continuous crossover, between a linear shear regime $v(r) \sim r$ for $r \ll 1$, and a regime at larger scale where the velocity difference between two points scales like $r^{1-\xi}$. The exponent ξ depends on the specific situation at hand; we have $\xi = 2/3$ in high-Reynolds-number turbulence, and $\xi = 1$ in porous media; however, the subsequent analysis holds for any $0 \le \xi \le 1$.

The velocity u is a representative root mean square velocity of a possibly time-dependent velocity, whose fluctuations give precisely rise to one particle dispersion [5,21]. The formulation in Eq. (7), which has no other fundamental justification than bridging two well-controlled scaling regimes through a simple crossover easily manipulable for further computations, is reminiscent of the one used by Kraichnan [22] for turbulence (i.e. a velocity rapidly fluctuating in time, but with a permanent spatial structure).

2.3. Arborescent growth

We first consider situations where the destruction term in the general population balance is zero. Then, Eq. (4) becomes

$$\partial_t N + v(r)\partial_r N = 0 \tag{10}$$

This conservation equation for $N(r,t)$ is strictly equivalent to a Liouville equation for the *density* of segments $n(r,t)$ such that $N(r,t) = \int_0^r n(r',t)\mathrm{d}r'$, or $n(r,t) = \partial_r N(r,t)$, which obeys

$$\partial_t n + \partial_r [v(r)\,n] = 0 \tag{11}$$

already used in this form in a different but related context [23].

It is clear that the dynamics in Eq. (10) has no stationary state. The r-elements are continuously stretched by the base flow, therefore providing room for ever more numerous smaller r-elements, and in the absence of destruction mechanism, their number grows in a multiplicative fashion as in Figs. 1a, b. When $v(r)$ is not a constant and depends on r, the r-elements are however unevenly stretched. This is easily figured out quantitatively by noticing that $\mathrm{d}\ln(e^{r^{\xi}} - 1)/\mathrm{d}r = \xi/[r^{1-\xi}(1 - e^{-r^{\xi}})]$ and by further scaling time t by

$$t \equiv \frac{u\,t}{d} \tag{12}$$

to obtain from Eq. (10)

$$\partial_t N + \partial_\psi N = 0, \quad \text{with} \quad \psi = \frac{1}{\xi}\ln\left(e^{r^{\xi}} - 1\right) \tag{13}$$

indicating that $N(\psi, t)$ now propagates at speed unity in the $\{\psi, t\}$ space, the $\psi - r$ transformation having compensated for the r-dependence of $v(r)$.

Solutions to Eq. (13) are of the form $N(r,t) = f[\ln(e^{r^{\xi}} - 1) - \xi t]$, for which the function $f[\cdot]$ is fixed by an initial condition. Imposing that the contour is initially smooth ($d_f = 1$), like in Figs. 1a, b for instance (we also set the initial blob size to d, without loss of generality), that is,

$$N(r, t = 0) = \frac{1}{r} \tag{14}$$
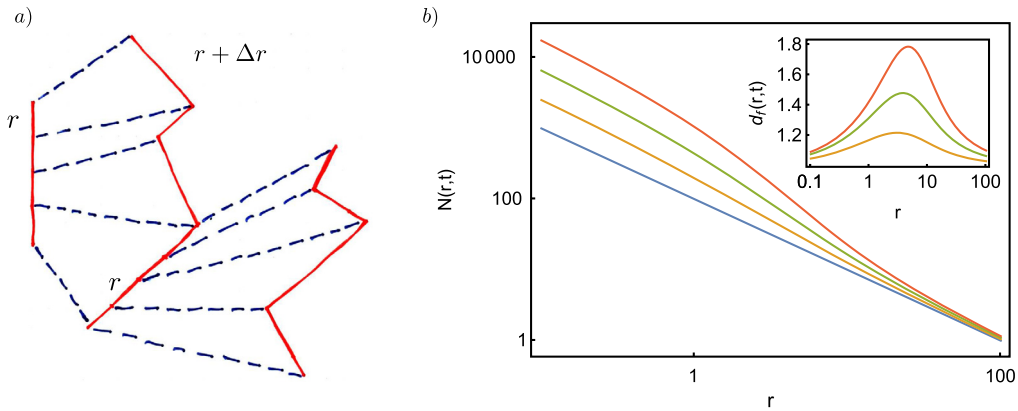
one has, at any posterior time t,

Fig. 2. a) Sketch of the arborescent pair dispersion process: each pair of material particles is stretched at velocity $v(r)$, dependent on r, thus corrugating the line. b) Number of segments $N(r,t)$ of size r needed to cover an initially smooth contour ($N(r,t=0) = 1/r$) for successive instants of time t according to (15) for $t = 0, 1, 2, 3$. Inset: the fractal dimension of the contour $d_f(r,t)$ versus r for the same times.

$$N(r,t) = \left\{ \ln\left[1 + e^{-\xi t}(e^{r^{\xi}} - 1) \right] \right\}^{-1/\xi} \tag{15}$$

hence illustrating, as seen in Fig. 2, how the material contour becomes *fractal* with a dimension

$$d_f(r,t) = -\frac{d \ln N(r,t)}{d \ln r} \tag{16}$$

depending both on scale, and time. The contour remains approximately smooth at small scale ($r \ll 1$), and gets progressively more corrugated for scales slightly larger than the crossover scale, thus reflecting the r-dependence of the underlying stirring law $v(r)$. The very large scales evolve at a slower pace (since $r/v(r) \sim r^{\xi}$ is an increasing function of r) and remain thus close to smooth (i.e. $d_f \approx 1$) for a longer time. Both the scale dependence of $d_f(r,t)$ [11] and its short-time increase [12,24, 13] are experimental facts, as long as new effects, discussed in the sequel, come into play.

The net material blob contour length

$$L(t) = \lim_{r \to 0} \{ rN(r,t) \} = e^{t} \tag{17}$$

increases exponentially in time because of the multiplicative nature of lengths stretching, as is common place in random or turbulent flows not dominated by a sustained shear [25–27]. Note that the net blob length $L(t)$ is fundamentally different from the end-to-end dispersion distance of the distorted contour $R(t)$, that is the distance separating the extreme ends of a stretched blob (see Fig. 1a). As soon as $R(t) \gg 1$, the integration of $\dot{R} = R^{1-\xi}$ given by (7) leads to

$$R(t) \sim t^{1/\xi} \tag{18}$$

independent of the initial size of the material contour, a relationship also known, with $\xi = 2/3$, as Richardson's law [8].

2.4. Global, r-independent decay

The burgeoning growth of material lines cannot go on indefinitely and there are several reasons for that. One is internal to the dynamics described above. The fractal dimension is predicted by Eq. (15) to increase with no bounds in time and thus to exceed the dimension of the embedding space (equal to 3 in the experiments shown in Fig. 1). Overlaps between adjacent sub-parts of the contour must necessarily occur, leading to the destruction of r-elements, and therefore to growth saturation.

Another reason is that we are describing the corrugation of objects that, as they are transported by the moving substrate, are likely to diffuse in it. The contours we are describing are borders of finite size lamella of substances carried by the flow (scalar dyes typically). A distorted scalar blob of dye *mixes* when it is stretched, meaning that its concentration starts, after some time, to decay. If the blob can be detected as long as the scalar concentration it carries remains above a threshold concentration c_s, then the time it takes for the contour to fade away and vanish in the diluting, stirred environment is of order (in units of d/u):

$$t_s \sim \ln\left(\frac{\sqrt{Pe}}{c_s} \right), \quad \text{where} \quad Pe = \frac{u\,d}{D} \tag{19}$$

is a Péclet number with D the molecular diffusion coefficient of the dye, a number usually large, but finite (see, e.g., [28, 29]).
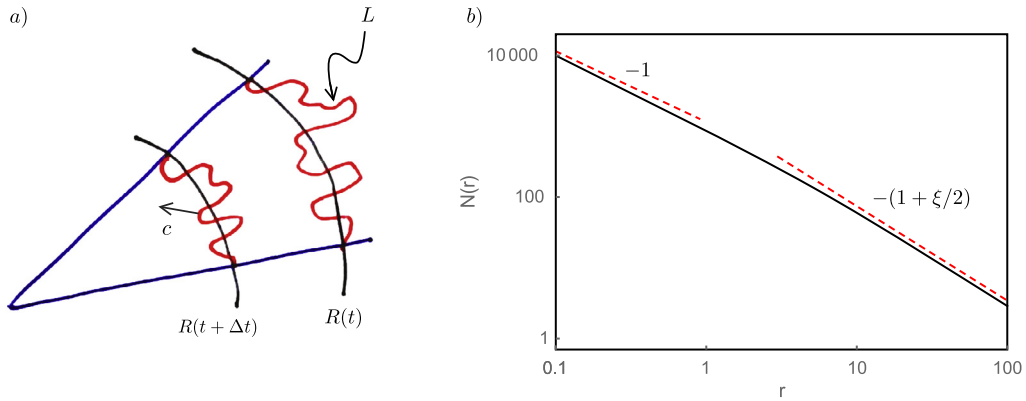
Fig. 3. a) Sketch of the destruction mechanism of r-elements on a self-propagating interface giving rise to the destruction rate in Eq. (24). The propagation velocity c is perpendicular to the interface. b) Stationary shape of the interface obtained from the integration of Eq. (26) with $\xi = 2/3$.

Let us consider first that the extinction time t_s above affects uniformly all the elements constitutive of the distorted lamella. The population balance dynamics of its contour now incorporates a loss term such that Eq. (3) becomes

$$N(r + \Delta r, t + \Delta t) = N(r, t) - N(r, t)\frac{\Delta t}{t_s} \tag{20}$$

or

$$\partial_t N + v(r)\partial_r N = -\frac{N}{t_s} \tag{21}$$

Setting $\tilde{N}(r, t) = N(r, t)\, e^{t/t_s}$, we have

$$\partial_t \tilde{N} + v(r)\partial_r \tilde{N} = 0 \tag{22}$$

which is, not surprisingly, formally identical to Eq. (10). A global, r-independent decay does not alter the relative proportion of the r-elements constitutive of the contour, but simply diminishes their overall number, proportionally to e^{-t/t_s}. This ingredient alone thus cannot account for the saturation of the fractal dimension. In fact, it should even be refined to incorporate the notoriously broad (exponential, see [28]) *distribution* of mixing times t_s in random flows of which Eq. (19) is a representative mean. To the longest mixing time in the distribution corresponds unmixed sub-parts of the lamella whose contour ultimately vanishes as a tiny segment. The fractal dimension, after the initial increase described in Section 2.3 for $t < t_s$ thus decreases down to close to 1 for $t > t_s$ [12,30], but no stationary state exist.

3. Propagating fronts: destruction of r-elements

Global scalar decay does not lead, as discussed above, to any kind of statistically steady interface shape. We consider now two ingredients for which interface creation and destruction actually balance.

3.1. Constant propagation velocity

Interfaces may propagate on their own. For instance, a flame is a thin out-of-equilibrium region separating a metastable bulk phase (the reactants) from a stable one (the products) and the return to equilibrium proceeds from the propagation of one phase into the other, at a velocity c locally perpendicular to the interface [31]. In that case, the interface is no more attached to tagged material particles in the stirring medium, but moves intrinsically through it. This phenomenon causes the destruction of r-elements in the following way.

Let R be the global extent of the interface (which may be the end-to-end distance of a distorted blob discussed in Eq. (18), or the diameter of the nozzle for a jet flame like in Fig. 1d, the size of the burner or the tube diameter in which the front propagates etc.), setting its typical radius of curvature. We discuss for simplicity the argument, illustrated in Fig. 3a, in two dimensions and we let the propagation be directed inwards.

Consider first a smooth circular interface of radius R, in the absence of stirring. The interface radius shrinks at constant speed $\dot{R} = -c$ and will vanish down to a point in a finite shrinking time R/c. We may also write equivalently $2\pi R\dot{R} = -Lc$ where $L = 2\pi R$ is the interface length. This relationship still holds when the interface is corrugated, as first noticed by G. Damköhler [32]. This explains why if L is larger than $2\pi R$, the interface speed $\dot{R}$ is increased relative to c by an amount L/R, which is proportional to the interface length, and thus why turbulent (and thus corrugated) flames propagate faster than laminar (straight) flames [33,34]. In our illustrated example of Fig. 3, the effective propagation speed $\dot{R}$ of the corrugated interface is thus such that

$$2\pi R\dot{R} = -Lc \tag{23}$$

where L is the net interface length measured at scales small enough for it to be r-independent (i.e. $r < d$), smooth, and thus propagating at speed c. With $L/R \sim (R/d)^{d_f-1}$, the propagation speed is anticipated to be $\dot{R} \sim c\,(R/d)^{d_f-1}$ (see, e.g., [35,36] and references therein).

We rewrite Eq. (23) at any scale r as $R\dot{R} \sim L(r)c(r)$. Both $\dot{R}$ and $c(r)$ are unknown at this stage, as well as d_f. Making use of Eqs. (1) and (2), which provide $\dot{N} = N(r)\dot{R}/R$, we find that the destruction rate of r-elements is

$$\dot{N}\big|_{\text{loss}} \sim rN^2 \frac{c(r)}{R^2} \tag{24}$$

a strongly decaying function of r (for a smooth interface in a medium at rest, $\dot{N}\big|_{\text{loss}} = c/r$).

The destruction speed of r-elements $c(r)$ is equal to c for a smooth contour as already stated, that is for corrugation scales r of the order of d or below, and is equal to zero for a straight interface propagating perpendicular to itself. In-between these two extremes and for an interface shrinking self-similarly in a time $R/\dot{R}$, the destruction speed $c(r)$ is such that the shrinking time $L(r)/c(r) = R/\dot{R}$ is independent of r, or

$$c(r) = \dot{R}\left(\frac{r}{R}\right)^{1-d_f} \tag{25}$$

a decaying function of r when $d_f > 1$, expressing consistently that small scale corrugations are erased faster than larger ones. As already noted, $c(r \ll d) \sim c$ since the interface is smooth there, within a logarithmic correction $\sqrt{\ln(u/c)}$ resulting from the Eikonal distortion of the front under stirring [37], accounting equivalently for the fact that no interface destruction occurs in the absence of intrinsic propagation, when $c = 0$.

Under stirring, the production term $v(r)\partial_r N$ in the general population balance in Eq. (4) competes with the above destruction term, and a steady state may now eventually be reached. The equilibrium is such that $v(r)\partial_r N = -\dot{N}\big|_{\text{loss}}$ and is described by

$$\partial_r\left(\frac{1}{N}\right) \sim \frac{r}{R^2}\frac{c(r)}{v(r)} \tag{26}$$

which solves for the stationary shape $N(r) \sim r^{-d_f}$, and self-consistently for the dimension d_f as a function of the stirring velocity exponent ξ. The asymptotic r-dependences of $N(r)$ are prescribed by those of $v(r)$ in Eq. (7). Setting $\mathcal{C} = c/u \times (d/R)^{2-\xi}$, we have (in scaled units):

$$N(r) \sim \frac{1}{\mathcal{C}\,r}, \quad \text{for } r \ll 1 \quad (\text{since } c(r \ll 1) = c, \text{ and } N(r \to 0) \to \infty) \tag{27}$$

$$N(r) \sim \frac{1}{\mathcal{C}\,r^{1+\xi/2}}, \quad \text{for } r \gg 1 \tag{28}$$

The interface is smooth at small scale, and fractal at larger scale, with dimension $d_f = 1 + \xi/2$. The crossover scale between these two extremes is at $r = 1$ independent of c and solely prescribed by the structure of the stirring field, while the net length of the interface $L = d\lim_{r\to 0}\{rN(r)\} = d\mathcal{C}^{-1}$ is proportional to the ratio of the stirring speed u to the intrinsic interface speed c. The mean interface speed (or combustion velocity) $\dot{R} = cL/R \sim u \times (R/d)^{1-\xi}$ is increased accordingly. It is, in this geometrical description, proportional to the stirring speed u, independent of c, as anticipated by Damköhler. A more refined description [37] would slightly alter this trend as

$$\dot{R} \sim \frac{u}{\sqrt{\ln(u/c)}}\left(\frac{R}{d}\right)^{1-\xi} \tag{29}$$

for which $\dot{R} \approx u$ when $u/c \gg 1$, but also $\dot{R} \to 0$ when $c \to 0$, as it should. The interface speed is a weakly increasing function of its global extent R, a fact known empirically [35,36].

3.2. Passive fronts: diffusive reconnections

We now come back to passively advected fronts, or at least fronts whose interface smears out by diffusion but which, when straight and smooth, do not propagate. We consider here the consequence of an ingredient already mentioned at the beginning of Section 2.4, namely the necessary overlaps that occur between adjacent sub-parts of the contour associated with the development of its corrugations.

A distorted blob in a free stirred environment like in Figs. 1a, c has a contour length $L(t)$ growing like $e^{\gamma t}$ (with $\gamma = u/d$), while its global extent $R(t)$ grows according to $t^{1/\xi}$ only (see Eqs. (17) and (18)). At some point, the blob interface is so convoluted and densely packed in space that the distance between adjacent portions of it become of the order of the diffusion length $\sqrt{D/\gamma}$. These reconnections are visible on the contour in Fig. 1c, composed of the intrication of two sources
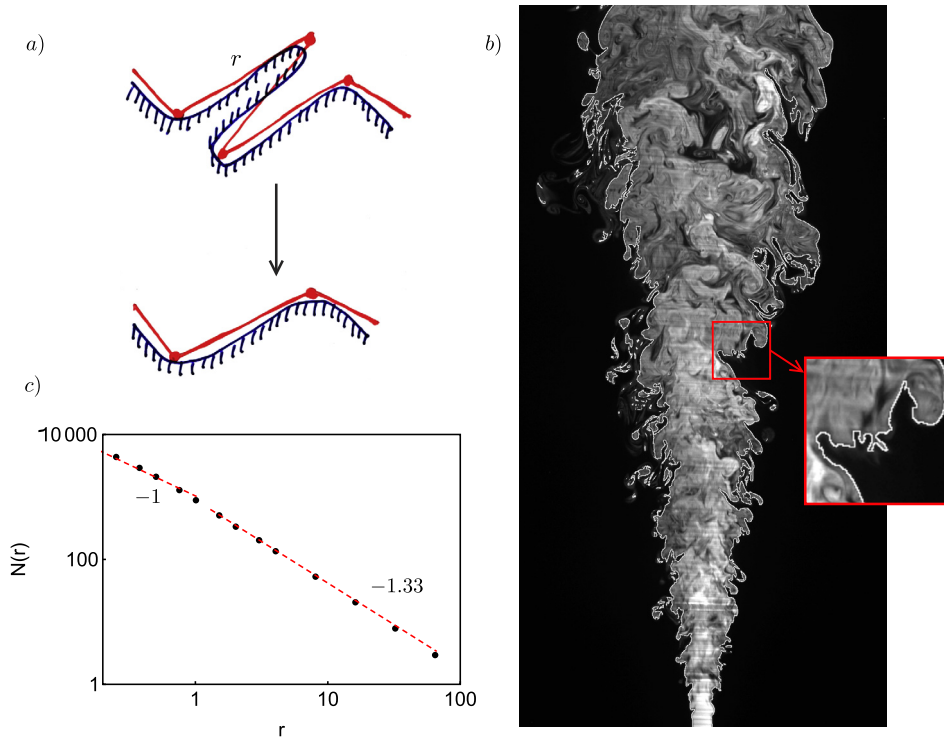
Fig. 4. a) Sketch of the diffusive coarsening mechanism leading the destruction of r-elements, thus limiting the interface growth. b) A planar cut through a water turbulent jet (diameter 4 mm at exit, Reynolds number 10^4) seeded with a weakly diffusing fluorescent dye. The interface of the jet with the still environment is the tiny white contour bordering the jet; it is highlighted in the inset. c) The number of segments $N(r)$ of size r needed to cover the contour in b). The crossover lengthscale $d = 1$ mm is of the order of the Taylor scale based on the transverse size of the jet at mid-height.

with distinct colors and displaying obvious overlaps. These overlaps are, besides, the key phenomenon to understand the structure of complex mixtures, and their rate of evolution towards uniformity [38]. Molecular diffusion smears the contours into a larger ensemble, called the *coarse grained scale* [39] given by, when written at scale r,

$$\eta(r) = r/\sqrt{Pe(r)} \tag{30}$$

$$= r\left(\frac{\gamma(r)r^2}{D}\right)^{-1/2} = \sqrt{\frac{D}{\gamma(r)}}, \quad \text{with} \quad \gamma(r) = v(r)/r \tag{31}$$

if $\gamma(r)$ is the stretching rate at scale r. Since the fusion process of an adjacent lamella on the contour takes a time on the order of $\gamma(r)^{-1}$ (times a weak correction function of the Péclet number, see Eq. (19)) and is accompanied by the disappearance of corresponding r-elements (typically $N(r) \to N(r)/3$ after fusion, see the sketch in Fig. 4a), the corresponding 'propagation speed' in the terminology of Section 3.1 is

$$c(r) = \gamma(r)\eta(r) = \sqrt{D\gamma(r)} \tag{32}$$

a decaying function of r because small scale corrugations overlap faster than larger ones. Adapting this new situation to the equilibrium between production and destruction of r-elements in Eq. (26), the stationary shape $N(r)$ is now ruled by

$$\partial_r\left(\frac{1}{N}\right) = \frac{1}{R^2}\sqrt{\frac{D}{\gamma(r)}} \tag{33}$$

The asymptotic r-dependences of $N(r)$ with r scaled by d as in Eq. (5) are, with $\mathcal{P} = (d/R)^2/\sqrt{Pe}$,

$$N(r) \sim \frac{1}{\mathcal{P}r}, \quad \text{for } r \ll 1 \tag{34}$$

$$N(r) \sim \frac{1}{\mathcal{P}r^{1+\xi/2}}, \quad \text{for } r \gg 1 \tag{35}$$

The net length of the interface $L = d \lim_{r\to 0}\{rN(r)\} = d\mathcal{P}^{-1}$ is larger if the interface is less diffusive, at larger Péclet number Pe.

The dimension of the interface for $r \gg 1$ is also, as for a self-propagating front, given by $d_f = 1 + \xi/2$ in that case. With $\xi = 2/3$ (and therefore $v(r) \sim r^{1/3}$ which suits to high Reynolds number turbulence), we find $d_f = 4/3$, a value commonly reported for turbulent interfaces, may they be self-propagating, or passively advected (see the review in [10]). Further illustrations are provided by the contour of a turbulent jet seeded with a weakly diffusing dye shown in Fig. 4, or by another type of diffuse interface with reconnections when the interface is reactive, undergoing a fast diffusion-controlled chemical reaction [4], as in Fig. 1d.

The existing interpretations for this known value of d_f are, however, very different from the present one. Inline with the orthodox theory of turbulence where dissipative effects are confined to small, cut-off scales but do not affect the inertial range of scales, $d_f = 4/3$ has received an inertial range interpretation 'à la Kolmogorov', or more exotic ones involving permanent coherent structures [40], all these scenarii being independent of molecular diffusion. Linking here the geometrical features of a distorted interface with its mixing kinetics, we show, on the contrary, that molecular diffusion operates, by the overlap mechanism, *at all scales*, a fact seldomly recognized (see, however, [22]). As long as diffusion has not set-in, that is, before the mixing time in Eq. (19), we have seen that $d_f(r, t)$ is a non-monotonous function of r, and increases in time t with no bounds. It is because interfaces are smeared by diffusion that their corrugations merge, percolate, and rectify. From this subtle equilibrium between interface creation and destruction by mixing, r-elements eventually self-organize in relative proportions $N(r)$ independent of time. The scaling features of $N(r)$ do not depend on the Péclet number Pe, but the net interface length L does.

4. Conclusion

We have provided a new, simple and unified framework to discuss the emergence of corrugations on material interfaces stirred by random media. Relating the shape of these interfaces to the process giving birth to it, we have formalized a population balance dynamics for the r-elements that cover the interface contour in the course of its deformation. As long as corrugations grow kinematically, shapes change continuously, their fractal dimension $d_f(r, t)$ is a non-monotonous function of the scale r, and increases in time t with no bounds. Interface creation and destruction balance in self-propagating fronts like flames, and in fronts smearing by molecular diffusion, through a mixing induced overlap mechanism, leading to a stationary shape. These findings, which help reexamining old observations, namely the fractal character of stirred interfaces, with a new perspective, also reconcile kinetics with geometry in showing why and when the latter depends on the former.

Acknowledgements

References

[1] B. Mandelbrot, On the geometry of homogeneous turbulence, with stress on the fractal dimension of the iso-surfaces of scalars, J. Fluid Mech. 72 (2) (1975) 401–416.

[2] P. Welander, Studies on the general development of motion in a two-dimensional, ideal fluid, Tellus 7 (2) (1955) 141–156.

[3] E. Villermaux, Y. Gagne, Line dispersion in homogeneous turbulence: stretching, fractal dimensions and micromixing, Phys. Rev. Lett. 73 (2) (1994) 252–255.

[4] E. Villermaux, Fast bimolecular reactions in high Reynolds number turbulence: structure of the reactive interface and surface of reaction, in: R. Benzi (Ed.), Advances in Turbulence V, Kluwer Academic Publishers, 1995, pp. 529–533.

[5] G.I. Taylor, Diffusion by continuous movements, Proc. Lond. Math. Soc. 20 (1921) 196–212.

[6] P. Langevin, Sur la théorie du mouvement brownien, C. R. Acad. Sci. Paris 146 (1908) 530–533.

[7] J. Duplat, S. Kheifets, T. Li, M.G. Raizen, E. Villermaux, Superdiffusive trajectories in Brownian motion, Phys. Rev. E 87 (2013) 020105.

[8] L.F. Richardson, Atmospheric diffusion shown on a distance-neighbour graph, Proc. R. Soc. Lond. A 110 (1926) 709–737.

[9] S. Corrsin, M. Karweit, Fluid line growth in grid-generated isotropic turbulence, J. Fluid Mech. 39 (1) (1969) 87–96.

[10] K.R. Sreenivasan, Fractals and multifractals in fluid turbulence, Annu. Rev. Fluid Mech. 23 (1991) 539–600.

[11] H.J. Catrakis, P.E. Dimotakis, Mixing in turbulent jets: scalar measures and isosurface geometry, J. Fluid Mech. 317 (1996) 369–406.

[12] E. Villermaux, C. Innocenti, On the geometry of turbulent mixing, J. Fluid Mech. 393 (1999) 123–145.

[13] F.C.G.A. Nicolleau, A. Elmaihy, Study of the development of three-dimensional sets of fluid particles and iso-concentration fields using kinematic simulation, J. Fluid Mech. 517 (2004) 229–249.

[14] J. Mantzaras, P.G. Felton, F.V. Bracco, Fractals and turbulent premixed engine flames, Combust. Flame 77 (1989) 295–310.

[15] B.D. Haslam, P.D. Ronney, Fractal properties of propagating fronts in a strongly stirred fluid, Phys. Fluids 7 (1995) 1931–1937.

[16] B. Denet, Fractal dimension of turbulent premixed flames for different turbulence spectra, Combust. Sci. Technol. 159 (2000) 305–314.

[17] R. Yu, X.-S. Bai, V. Bychkov, Fractal flame structure due to the hydrodynamic Darrieus–Landau instability, Phys. Rev. E 92 (2015) 063028.

[18] J. Kalda, Simple model of intermittent passive scalar turbulence, Phys. Rev. Lett. 84 (3) (2000) 471–474.

[19] P. Meunier, E. Villermaux, The diffusive strip method for scalar mixing in two-dimensions, J. Fluid Mech. 662 (2010) 134–172.

[20] M. Kree, E. Villermaux, Scalar mixtures in porous media, Phys. Rev. Fluids 2 (2017) 104502.

[21] R.H. Kraichnan, Small-scale structure of a scalar field convected by turbulence, Phys. Fluids 11 (5) (1968) 945–953.

[22] R.H. Kraichnan, Anomalous scaling of a randomly advected passive scalar, Phys. Rev. Lett. 72 (1994) 1016.

[23] J.-C. Geminard, P. Pelcé, Statistical approach for radial fingering in a Hele Shaw cell, J. Phys. II 2 (1992) 1931–1940.

[24] E. Villermaux, H. Rehab, Mixing in coaxial jets, J. Fluid Mech. 425 (2000) 161–185.

[25] W.J. Cocke, Turbulent hydrodynamic line stretching: consequences of isotropy, Phys. Fluids 12 (12) (1969) 2488–2492.

[26] S. Kida, S. Goto, Line statistics: stretching rate of passive lines in turbulence, Phys. Fluids 14 (1) (2002) 352–361.

[27] M. Souzy, H. Lhuissier, E. Villermaux, B. Metzger, Stretching and mixing in sheared particulate suspensions, J. Fluid Mech. 812 (2017) 611–635.

[28] B.I. Shraiman, E.D. Siggia, Scalar turbulence, Nature 405 (2000) 639–646.

[29] E. Villermaux, Mixing versus stirring, Annu. Rev. Fluid Mech. (2019), https://doi.org/10.1146/annurev-fluid-010518-040306.

[30] J. Schumacher, K.R. Sreenivasan, Geometric features of the mixing of passive scalars at high Schmidt numbers, Phys. Rev. Lett. 91 (17) (2003) 174501.

[31] P. Clavin, G. Searby, Combustion Waves and Fronts in Flows, Cambridge University Press, 2016.

[32] G. Damköhler, Der Einfluss der Turbulenz auf die Flammengeschwindigkeit in Gasgemischen, Z. Elektrochem. 46 (11) (1940) 601–652.

[33] W.R. Hawthorne, D.S. Wendell, H.C. Hottel, Mixing and combustion in turbulent gas jets, in: Proc. Third Symposium on Combustion and Flame and Explosion Phenomena, Baltimore, MD, USA, 1949, pp. 266–288.

[34] R.G. Abdel-Gayed, D. Bradley, M. Lawnes, Turbulent burning velocities: a general correlation in terms of straining rates, Proc. R. Soc. Lond. A 414 (1987) 389–413.

[35] N. Vladimirova, P. Constantin, A. Kiselev, O. Ruchayskiy, L. Ryzhik, Flame enhancement and quenching in fluid flows, Combust. Theory Model. 7 (2003) 487–508.

[36] J. Quinard, G. Searby, B. Denet, J. Grana, Self-turbulent flame speeds, Flow Turbul. Combust. 89 (2) (2012) 231–247.

[37] V. Yakhot, Propagation velocity of premixed turbulent flames, Combust. Sci. Technol. 60 (1–3) (1988) 191–214.

[38] T. Le Borgne, P.D. Huck, M. Dentz, E. Villermaux, Scalar gradients in stirred mixtures and the deconstruction of random fields, J. Fluid Mech. 812 (2017) 578–610.

[39] E. Villermaux, J. Duplat, Coarse grained scale of turbulent mixtures, Phys. Rev. Lett. 97 (2006) 144506.

[40] J.C.H. Fung, J.C. Vassilicos, Fractal dimensions of lines in chaotic advection, Phys. Fluids A 3 (1995) 2725–2733.